doi:10.1016/j.jmb.2004.09.055 J. Mol. Biol. (2004) 344, 813–826

JMB

Available online at www.sciencedirect.com

SCIENCE DIRECT®

ELSEVIER

Independent ATPase Activity of Hsp90 Subunits Creates a Flexible Assembly Platform

Stephen H. McLaughlin*, Laure-Anne Ventouras, Bastiaan Lobbezoo and Sophie E. Jackson*

Cambridge University Chemical Laboratory, Lensfield Road Cambridge CB2 1EW, UK

*Corresponding authors

The ATPase activity of the molecular chaperone Hsp90 is essential for its function in the assembly of client proteins. To understand the mechanism of human Hsp90, we have carried out a detailed kinetic analysis of ATP binding, hydrolysis and product release. ATP binds rapidly in a two-step process involving the formation of a diffusion–collision complex followed by a conformational change. The rate-determining step was shown to be ATP hydrolysis and not subsequent ADP dissociation. There was no evidence from any of the biophysical measurements for cooperativity in either nucleotide binding or hydrolysis for the dimeric protein. A monomeric fragment, lacking the C-terminal dimerisation domain, showed no dependence on protein concentration and, therefore, subunit association for activity. The thermodynamic linkage between client protein binding and nucleotide affinity revealed ATP bound Hsp90 has a higher affinity for client proteins than the ADP bound form. The kinetics are consistent with independent Michaelis–Menten catalysis in each subunit of the Hsp90 dimer. We propose that Hsp90 functions in an open-ring configuration for client protein activation.

Keywords: molecular chaperone; Hsp90; heat shock; protein folding; geldanamycin

Introduction

Hsp90 assists in the activation of a wide range of proteins (termed client proteins), including many involved in signaling and transcription[1–4] by a mechanism dependent on its ability to bind and hydrolyse ATP.[5,6] The rate at which it cycles is critical with hyper- and hypo-activity compromising function *in vivo*.[7] The ATPase activity is regulated by the transient association of Hsp90 with a variety of co-chaperones[8–11] as well as by the binding of client proteins.[10] The ATPase activity of Hsp90 is inhibited by the ansamycin anti-tumour drugs, that bind at the ATP-binding site,[12] leading to the degradation of Hsp90-associated oncogenic signalling proteins.[13] It follows that the status of the N-terminal nucleotide binding domains[6,14] must be linked to the properties of other domains involved in client protein and co-chaperone interaction.

The molecular mechanism by which ATP turnover regulates Hsp90 is unclear at present. Hsp90 is a multi-domain protein consisting of three domains: an N-terminal ATP-binding domain; a middle region; and a C-terminal homodimerisation domain containing a TPR-protein binding motif.[2] ATP binding changes the global properties of the protein such as a reduction in hydrophobicity[15] implying conformational changes or domain reorganization. As structural information on full-length Hsp90 has so far been frustrated by the lack of good diffraction data, the experimental evidence for the conformational changes that ATP binding elicits in Hsp90 has been interpreted in light of data from other members of the GHKL family of ATPases, such as DNA Gyrase B and MutL which contain structurally homologous ATP-domains.[16] Central to current models of Hsp90 action[7,10,17] (Figure 1) is that binding of ATP in the N-terminal domains

Present address: L.-A. Ventouras, Wellesley College, Wellesley, MA, USA.

Abbreviations used: ITC, isothermal titration calorimetry; GR-LBD, glucocorticoid receptor ligand-binding domain; SAXS, small-angle X-ray scattering; MDCC, *N*-[2-(1-maleimidyl)ethyl]-7-(diethylamino)-coumarin-3-carboxamide; DTT, dithioreitol; EDTA, ethylene diaminetetraacetic acid.

E-mail addresses of the corresponding authors: shm25@cam.ac.uk; sej13@cam.ac.uk

0022-2836/$ - see front matter

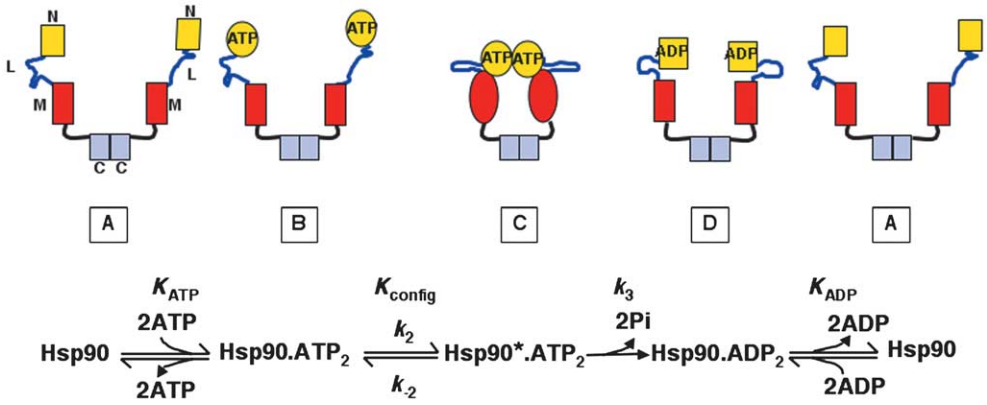

Figure 1. Current model of the mechanism of Hsp90 ATPase activity. Each subunit in the Hsp90 homodimer consists of three domains: N-terminal nucleotide binding domain (N), middle domain (M), separated by a flexible charged linker region (L), and a C-terminal dimerisation domain (C). The model proposes that ATP binding (state A to B) causes large conformational changes resulting in the transient association of the N domains (state C)[7,17] so encapsulating a client protein between the walls of the subunits. Intra-subunit N and M domain interactions are important for actvity.[19] ATP hydrolysis causes dissociation of the N-terminal domains allowing release of the client protein (state D). Dissociation of ADP recycles Hsp90 to its initial state (A). The kinetics of hydrolysis will depend on the binding of two molecules of ATP per dimer. In this model, a kinetic intermediate should be apparent as the Michaelis–Menten constant K_m will not be equal K_{ATP} but also depend on the value of K_{config} if k_{-2} is equal to or smaller than k_3. For yeast Hsp90, it is uncertain whether the rate-limiting step in the cycle is the formation of the N-terminal dimer or the hydrolysis step.

drives their self-association in a similar fashion to DNA Gyrase.[18] A dimerisation interface is proposed to be formed by the exposure of a hydrophobic surface on the N-terminal domains when the "ATP-lid" closes over the occupied nucleotide-binding pocket. N-terminal dimerisation commits Hsp90 to hydrolysis, which depends upon contacts between the N-terminal domain and the middle domain[19] in a similar manner to DNA Gyrase.[18] Closure of the N-terminal domains is proposed to capture a client protein in a "molecular clamp" within the wall of the closed ring. Subsequent ATP hydrolysis breaks the ring at the N-terminal dimerisation interface allowing escape of the client protein. This led to the proposal that the ATP turnover rate governs the time that a client protein remains bound by Hsp90.[7,10,20]

Although, Hsp90 undergoes several conformational changes in the current model, previous kinetic studies on yeast Hsp90 detected the presence of a single intermediate step after ATP binding prior to hydrolysis.[7,17] There is debate as to whether N-terminal dimerisation or the hydrolysis step itself is rate-limiting for the ATPase activity (Figure 1).[7,17] In addition, it is unkown why human Hsp90 is a much weaker ATPase than the yeast homologue.[10] It is possible that a different step in the cycle could be rate-limiting as a result of: (i) a shift in the equilibrium of the conformational change; (ii) a much slower rate of hydrolysis; or (iii) a slower rate of ADP dissociation.

The steady-state ATPase activity of human and yeast Hsp90 can be fitted by simple Michaelis–Menten kinetics.[5,6,10] Such simplicity is in conflict with the N-terminal homodimerisation model for ATP-driven Hsp90 function. It might be expected that two molecules of ATP per dimer would have to be simultaneously bound for any activity (Figure 1) leading to a dependence on the square of the substrate concentration. The possibility of a second ATP-binding site in the C-terminal region which has been proposed by several groups[21,22] would also lead to further complications in any kinetic scheme. To unravel these contradictions, we have dissected the kinetic mechanism of human Hsp90 ATPase activity to reveal the dynamics of the individual steps in binding and hydrolysis, leading us to propose a new model of Hsp90 function.

Results

Nucleotide affinity of human Hsp90

Recently, it has been suggested that in addition to the N-terminal nucleotide-binding domain, the C-terminal domain of Hsp90 can also bind ATP[21,22] and novobiocin, an inhibitor of DNA Gyrase B.[23] Therefore, as a basis for the subsequent kinetic analysis, the stoichiometry and binding constants of the interactions of the non-hydrolysable ATP analogue AMP-PNP and ADP with human Hsp90 were determined by isothermal titration calorimetry (ITC) at 25 °C (Figure 2). When data were fitted with three floating variables: stoichiometry; dissociation binding constant, K_d; and the change in enthalpy of interaction, AMP-PNP was determined to bind with a dissociation constant, K_d of 148($\pm$12) μM at a stoichiometry of 1.2$\pm$0.3 to each Hsp90 subunit. ADP bound more tightly with a K_d of 7.2($\pm$0.3) μM at a stoichiometry of 0.77$\pm$0.1. Constraining the analysis of the data by fixing the stoichiometries at values higher than one did not give accurate fits (data not shown). Using a higher concentration of ADP where Hsp90 was saturated after a lower number of injections, no second

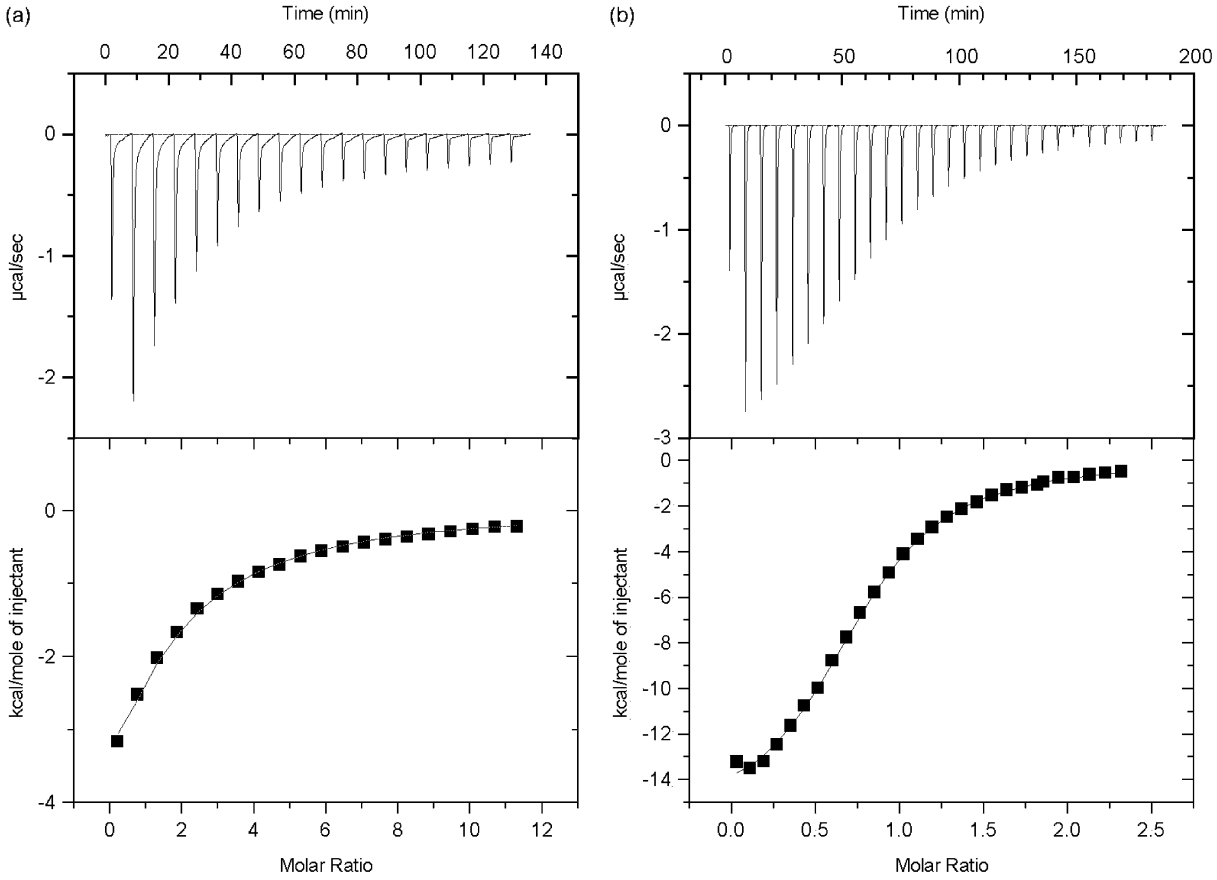

Figure 2. Isothermal titration calorimetry of nucleotide binding to Hsp90. AMP-PNP (a) and ADP (b) were injected into a cell containing full-length Hsp90 at 25 °C. Both nucleotides bound with stoichiometries of approximately 1 : 1 with K_d of 148(±12) μM and 7.2(±0.3) μM for AMP-PNP and ADP, respectively.

binding event was apparent (data not shown). As a consequence, it is assumed in all further kinetic analysis that Hsp90 possesses one nucleotide-binding site per subunit.

Binding of nucleotides was accompanied by a decrease in the intrinsic fluorescence of Hsp90 (Figure 3). The same fractional change in fluorescence was observed for all nucleotides at saturating concentrations (data not shown). The decrease in fluorescence due to the absorbance of incident light by increasing concentration of nucleotides was minimised by exciting at 295 nm and correcting the raw data for the inner-filter effect using equation (1). Corrected data were fitted to a single-binding model using equations (2) and (3) to calculate values for K_d for AMP-PNP and ADP (Figure 3(a) and (c), respectively) of 157(±12) μM and 7.4(±1.1) μM at 25 °C. These values agree well with those obtained by ITC, so validating intrinsic fluorescence as an accurate probe of nucleotide binding. Analysis of the binding using a two-site model based on the Adair equation[24] did not give significantly different values for the two calculated binding constants. An increase in temperature to 37 °C decreased the affinity for AMP-PMP to 790(±45) μM (data not shown) close to the measured Michaelis–Menten binding constant of 840 μM[10] and decreased the affinity for ADP to 41(±6) μM (data not shown). ATP bound with a slightly weaker affinity than its non-hydrolysable analogue with a K_d of 240(±14) μM (Figure 2(b)) at 25 °C. In the presence of a client protein, the glucocorticoid receptor ligand-binding domain (GR-LBD), there was a marked change in the fluorescence titration curves for ATP and its non-hydrolysable analogue AMP-PNP (Figure 3(a) and (b)). This was not due to the fluorescence of the client protein reporting on the client protein interaction directly as the maximum change in fluorescence, in the presence and absence of GR-LBD, remained unchanged. The presence of the client protein increased the affinity for ATP and AMP-PNP (seen as a left-shift in the binding curves in Figure 3(a) and (b)) with a corresponding decrease in K_d to 15(±1) μM and 7.4(±0.9) μM, respectively. GR-LBD exerts the opposite effect on Hsp90 ADP affinity, inducing an increase in K_d to 41(±4) μM at 25 °C (Figure 3(c)).

The binding of ATP to the N-terminal domains of Hsp90 is proposed to induce dimerisation of the domains (Figure 1).[7] It would be expected that such an interaction would stabilise the binding of ATP in both sites leading to a higher affinity with both sites occupied by ATP compared with the binding to a single site. Therefore, to probe for the cooperativity of nucleotide binding, the fluorescence binding data were transformed using the Hill-like equation (4)

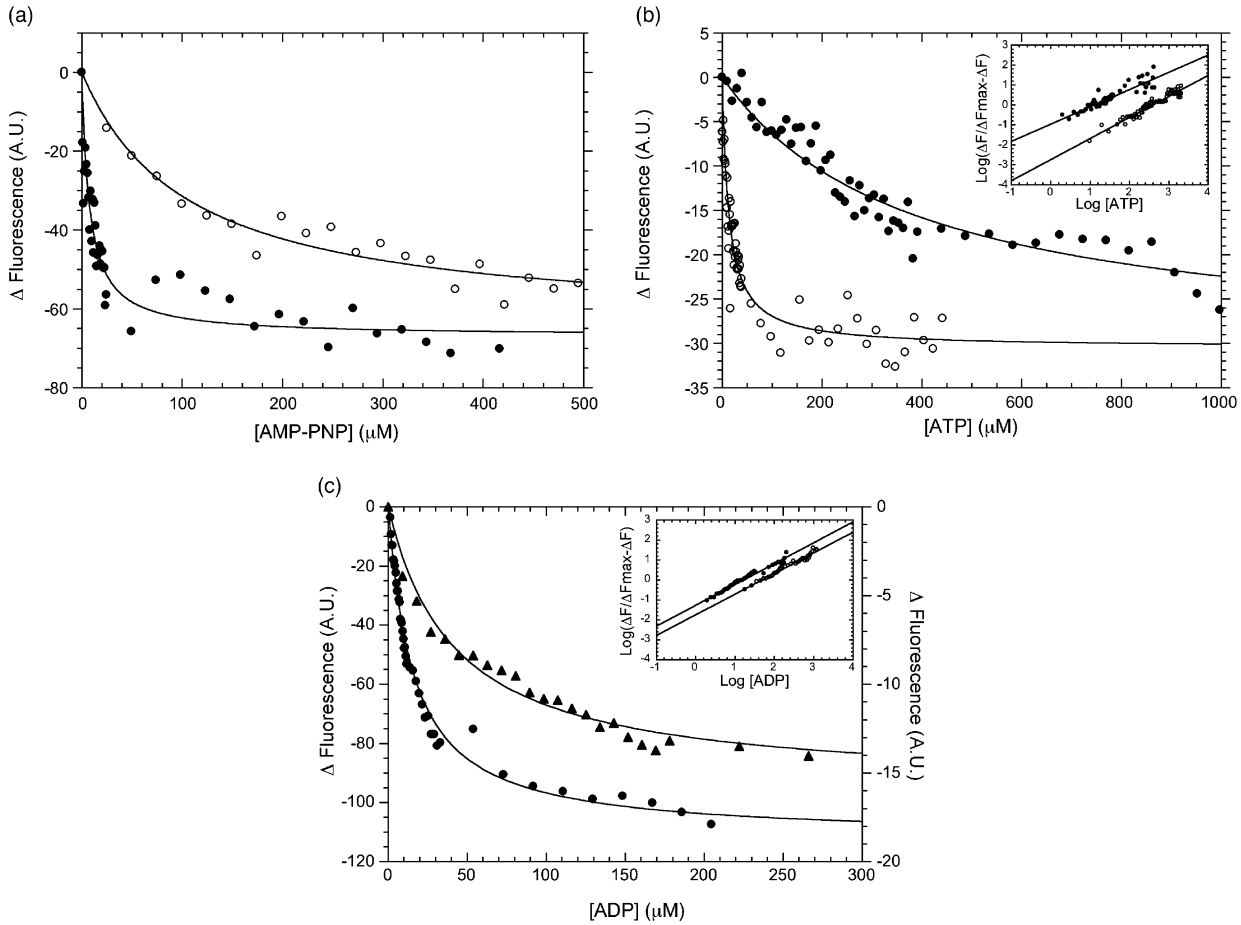

Figure 3. Equilibrium nucleotide binding affinities of Hsp90. Nucleotides were titrated into 2 μM Hsp90, in the absence and presence of 2 μM GR-LBD, and changes in the intrinsic fluorescence of Hsp90 measured at 25 °C. After correcting for the inner-filter effect of added nucleotides, data were fitted to a simple single-binding site model for (a) AMP-PNP in the absence (○) and presence of GR-LBD (●); (b) ATP in the absence (●) and presence of GR-LBD (○); and (c) ADP in the absence (●) and presence of GR-LBD (▲). Binding data were transformed and fitted to a Hill equation (4), insets in (b) and (c) giving a cooperativity constant of close to 1.

(Figure 3(b) and (c), insets). The gradient of the linear fits represent the degree of cooperativity. For both ATP and ADP, in the presence and absence of GR-LBD, the gradient is 1.0 ± 0.1, indicating there is no cooperativity in nucleotide binding.

Kinetics of nucleotide binding

To identify the rate-limiting step in the Hsp90 ATPase cycle, the kinetics of ATP binding, hydrolysis and subsequent ADP dissociation were determined. Taking advantage of the fluorescence change in Hsp90 upon nucleotide binding, the individual rate constants were measured by stopped-flow fluorescence. Upon mixing of Hsp90 and nucleotide the fluorescence decreased exponentially within the millisecond to second timeframe (Figure 4(a), upper trace). The fluorescence data fitted best to a single exponential function with linear drift as judged by the residuals after subtracting the fit from the data (Figure 4(a), lower trace). Over longer time-frames, no other phases were apparent with the fluorescence decreasing due to drift and photobleaching, at a rate independent of added nucleotide (data not shown). Consequently, in the initial analysis, a simple model was used as it was assumed the fluorescence data report on a single-binding step between Hsp90 and nucleotide. Hence, the observed rate constants at different concentrations of nucleotide and temperatures were fitted to a simple linear equation: $k_{obs} = k_{on}[L] + k_{off}$, where [L] is the concentration of nucleotide. The intercept of the plot gives the dissociation rate constant (k_{off}) and the gradient the rate constant of association (k_{on}). For the simple, single-step binding model, the on-rate constant for ADP was $3.7 \times 10^5\ M^{-1}\ s^{-1}$ with an off-rate constant of approximately $3\ s^{-1}$ at 25 °C (Figure 4(b)). The ratio of these two rate constants is 7.2 μM equal to the equilibrium dissociation constant ($K_d = k_{off}/k_{on}$). The on-rate constant for AMP-PNP was $5.6 \times 10^4\ M^{-1}\ s^{-1}$ compared to $1.0 \times 10^5\ M^{-1}\ s^{-1}$ for ATP at 10 °C (Figure 4(c)) with off-rate constants of $4.5\ s^{-1}$ and $16.3\ s^{-1}$, respectively. An increase in the temperature to 25 °C doubled the on-rate for ATP to $2.3 \times 10^5\ M^{-1}\ s^{-1}$

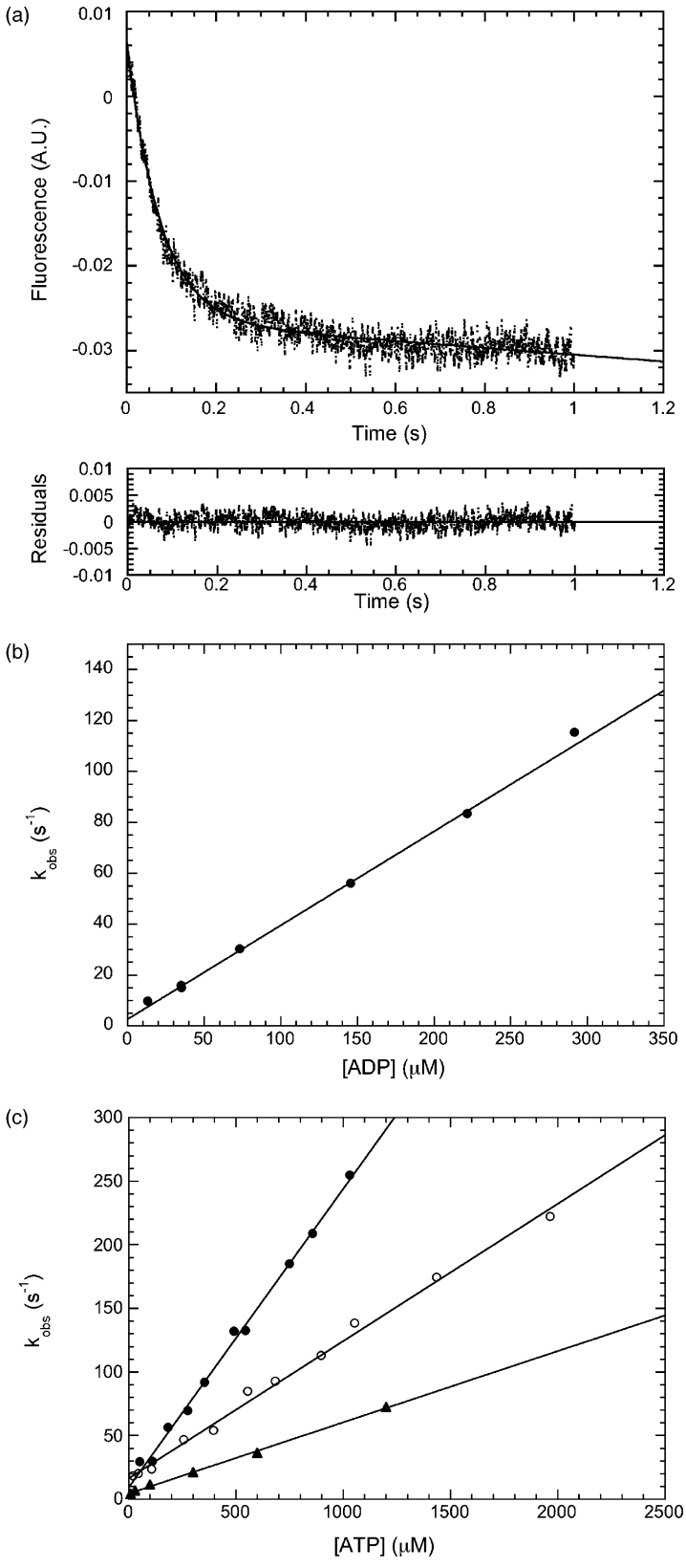

Figure 4. Pre-steady state nucleotide binding kinetics. (a) The change in fluorescence after mixing of ADP and Hsp90 was measured by stopped-flow fluorimetry. Data were fitted to a single exponential with linear drift (upper trace) as this gave the best values for the residuals (lower trace). The observed rates at different concentrations of (b) ADP at 25 °C, (c) AMP-PNP at 10 °C (▲), ATP at 10 °C (○) and 25 °C (●) were fitted by linear least squares.

within the same range as ADP. The off-rate constant, under these conditions, for ATP was 9 s^{-1}.

For both AMP-PNP and ADP there was an excellent agreement between $K_{d\ kin}$ and $K_{d\ eqm}$. For ATP, $K_{d\ kin}$ is approximately one-half to one-sixth the value of the equilibrium constants at 10 °C and 25 °C, respectively. The apparent difference in the kinetic and equilibrium values for ATP may indicate that, in contrast to its non-hydrolysable analogue AMP-PNP, ATP is undergoing hydrolysis

during the binding experiments. Alternatively, the difference may indicate there is another step in binding nucleotides.

Kinetics of ATP hydrolysis

It has been proposed for the yeast protein that either a conformational change prior to the hydrolysis step or the hydrolysis itself is rate limiting for Hsp90 ATPase activity.[17] To investigate if there are any intermediates on the kinetic pathway of human Hsp90 ATPase activity and to determine the rate-limiting step in the reaction, the steady-state kinetics of ATP hydrolysis were compared with activity under single-turnover conditions. Theory predicts that the presence of an intermediate in the pathway (as in Figure 1) will have two effects on the Michaelis–Menten steady-state parameters if k_{-2} is equal to or smaller than k_3: (i) k_{cat} is reduced by a factor of $K/(1+K)$, where K is the equilibrium constant for the formation of the intermediate and (ii) K_m will be lower than the substrate dissociation constant by a factor of $(1+K)$. Under single-turnover conditions, the hydrolysis rate constant was measured to be $7(\pm1)\times10^{-5}\,s^{-1}$ (Figure 5, filled circles) which is almost identical with the steady-state rate constant of $9.2(\pm0.2)\times10^{-5}\,s^{-1}$ at 25 °C (Figure 5, open circles). There was a negligible increase in ATP breakdown in the absence of Hsp90 (data not shown). Under steady-state conditions, the K_m was 190($\pm$20) μM at 25 °C (data not shown) similar to the measured dissociation constant of 240 μM (Figure 3). Hence, no intermediate step between the initial ligand-binding and hydrolysis is kinetically apparent. Taken together with the much higher rate of product dissociation (Figure 4(b)), the cleavage of ATP is the rate-limiting step in the Hsp90 ATPase cycle.

Cooperativity of Hsp90 ATPase activity

The ATPase activity of Hsp90 has been proposed to be activated like other members of the GHKL family by both inter- and intra-subunit interactions.[7,19] The N-terminal fragments of nucleotide-bound DNA Grase B[18] and MutL[25] are dimers in their respective crystal structures. Subsequently, the importance of N-terminal dimerisation in the catalytic mechanism of ATP hydrolysis by DNA Gyrase B was confirmed by the non-linear dependence of activity on concentration of the monomeric N-terminal fragments.[26] To ascertain if human Hsp90 displays a similar dependence on N-terminal dimerisation, the C-terminal homodimerisation domain was removed to generate a monomeric fragment. This was achieved by introducing a stop codon after the region coding for the middle domain.[19]

The oligomeric status of the purified fragment consisting of the N-terminal and middle domain, Hsp90ΔC (1–536), was determined by size-exclusion chromatography. In the presence of ATP, Hsp90ΔC eluted as a monomer over a concentration range of 3–69 μM (Figure 6(a)). If there is a fast exchange between a monomer and dimer, a shift in the position of elution might not be apparent. To trap any potential dimers, this construct (at a concentration of 63 μM in the presence and absence of AMP-PNP and ADP) was treated with an excess concentration of the chemical cross-linker DSS using conditions that can trap weak interactions in cells.[27] Analysis of the reaction by SDS-PAGE failed to show the presence of significant amounts of any cross-linked dimeric products (data not shown).

The fragment displayed apparent Michaelis–Menten kinetics at 37 °C (Figure 6(b)) with a tenfold lower catalytic rate constant ($1.2\times10^{-4}\,s^{-1}$) and threefold decrease in K_m (230($\pm$10) μM) compared to full-length Hsp90. The increased affinity for nucleotide of the truncated Hsp90 compared to the full-length was confirmed by the approximate twofold decrease in the dissociation constant for AMP-PNP (80($\pm$40) μM) at 25 °C as measured by a fluorescence titration experiment (data not shown).

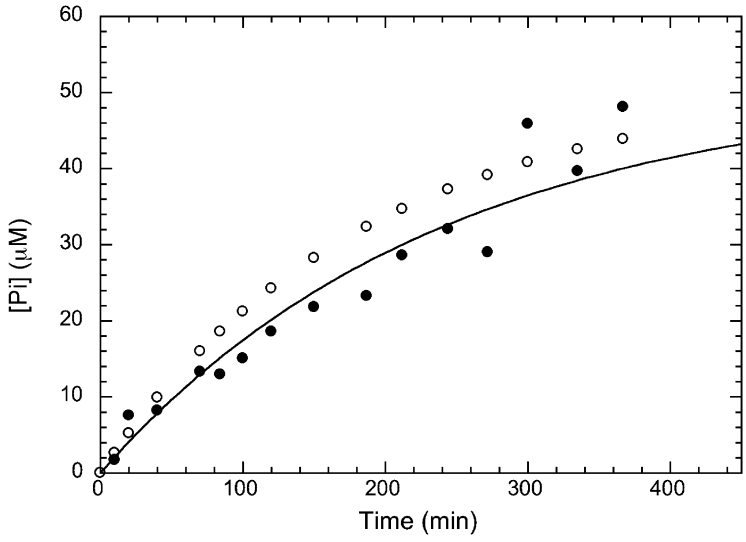

Figure 5. Single-turnover ATPase activity. ATP was added at a final concentration of 100 μM to a 100 μl reaction with or without 250 μM Hsp90 at 25 °C. At timepoints, an aliquot was removed and quenched with 20 mM EDTA on ice. The inorganic phosphate released was measured and corrected for the background (●). Data were fitted to a single exponential equation (5) and compared to the expected values from the steady-state rate (○).

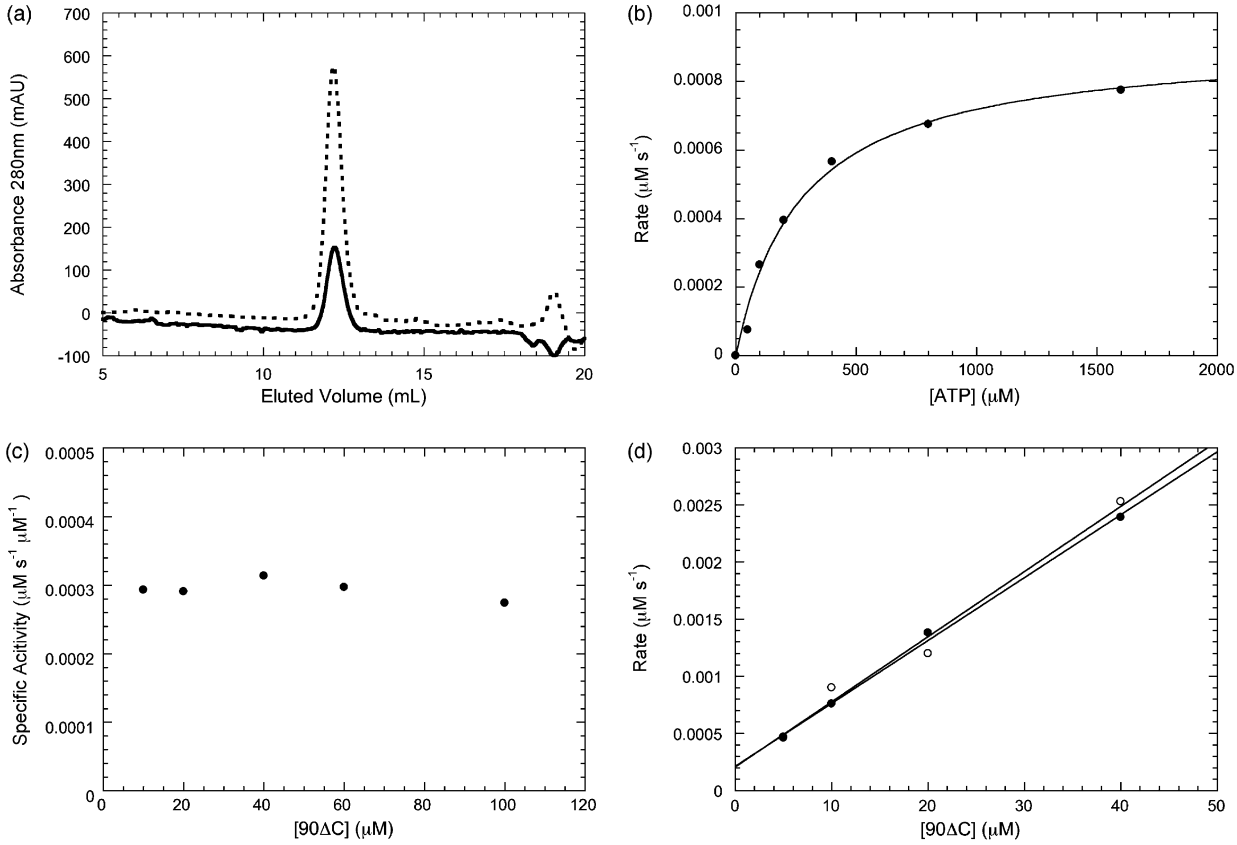

Figure 6. Effect of C-terminal truncation of Hsp90 on association and activity. (a) The oligomeric status of 10 μM (continuous line) and 69 μM (broken line) Hsp90ΔC were examined by gel filtration on a Sephadex 200 HR10/30 column. Molecular masses were calculated by comparing the relative elution (equation (6)) with those of standard proteins. (b) Steady-state ATPase activity of 10 μM Hsp90ΔC at 37 °C was fitted to Michaelis–Menten kinetics. (c) Variation of specific activity with increasing Hsp90ΔC concentrations. (d) The effect of increasing Hsp90ΔC concentration on ATPase activity in the absence (○) and presence of 10 μM GR-LBD (●).

To examine for any apparent dimerisation, the rate of ATP hydrolysis was examined over a wide protein concentration range. ATPase assays were carried out in the presence of 10% (v/v) glycerol to stabilise Hsp90ΔC. Addition of glycerol did not affect the ATPase rate of full-length Hsp90 or stimulation by binding of GR-LBD (data not shown). The specific activity of Hsp90ΔC was unchanged up to a concentration of 100 μM (Figure 6(c)), indicating no apparent dimerisation within the concentration range tested.

The ATPase activity of human Hsp90 and yeast Hsp90 have been shown to be specifically stimulated by a client protein, GR-LBD.[10] The molecular mechanism by which GR-LBD stimulates the catalytic rate is unknown. One possibility is that the hydrophobic protein binds to the middle domains of Hsp90, passively bringing the two N-terminal domains closer together, so increasing the rate of N-terminal dimerisation. If this is the case, then the client protein should then stimulate the activity of Hsp90ΔC and also induce a dimeric protein concentration dependence. Surprisingly, the presence of the client protein had no effect on the Hsp90ΔC ATPase activity and, in addition, did not effect the linear dependence of activity on protein concentration (Figure 6(d)).

It is possible that the lack of an apparent association between the N-terminal domains of Hsp90ΔC is due to a very weak affinity between the domains (i.e. in the millimolar range) that could not be probed at the concentrations used in our experiments. In the context of the full-length dimeric protein, however, the low affinity would be overcome as the formation of a homodimer *via* the C-terminal domains would increase the effective concentration of the two N-terminal domains. This mechanism would predict the presence of cooperativity in the hydrolysis of ATP or, at the very least, a dependence of two ATP molecules simultaneously binding to each homodimer for hydrolysis to occur. This was examined by transforming the initial rates of Hsp90 ATP hydrolysis at different ATP concentrations in terms of fraction of maximum activity and fitting to the Hill-like equation (4). The gradient of the data plotted in Figure 7 measures the degree of cooperativity in activity at 25 °C. For both the basal ATPase rate and the rate stimulated by the presence of the client protein GR-LBD, the gradient is 1.0 ± 0.1, indicating the absence of cooperativity

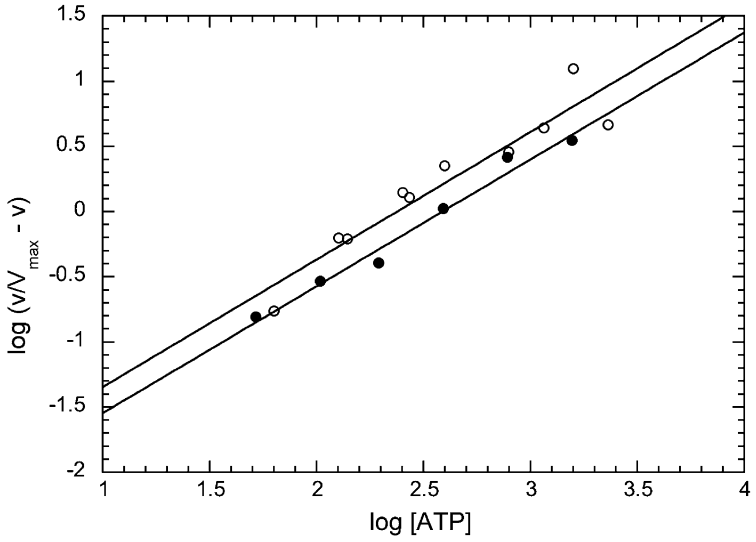

Figure 7. Cooperativity of Hsp90 ATPase activity. The steady-state ATPase activity (v) of full-length Hsp90 in the absence (●) and presence of GR-LBD (○), at 25 °C, were transformed to fractional rates ($v/V_{max}-v$), where V_{max} is the Michaelis–Menten constant, so as to fit to Hill-like equation (4). The gradient of the plot gives the degree of cooperativity.

and confirming the dependence of one ATP molecule binding per subunit for activity. A similar result was obtained using basal and stimulated activity, measured at 37 °C.[10]

Discussion

Here, we have sought to understand the mechanism of Hsp90 function in molecular terms by examining the precise steps in the kinetics of ATP binding and hydrolysis and linking these to the affinity of Hsp90 for a client protein. Our results suggest a new model for the ATPase cycle of human Hsp90 compared to the current model for the yeast protein in which ATP-induced N-terminal dimerisation is an obligate step. For human Hsp90, such a step could not be confirmed in the pathway by either: the observation of (i) cooperativity in nucleotide binding or hydrolysis; or (ii) the protein concentration dependence on dimerisation for activity of monomeric Hsp90ΔC. We will consider each of the individual steps in the human Hsp90 ATPase cycle and how these relate to its function in client protein activation.

Conformational changes after nucleotide binding to Hsp90

Nucleotide binding is a simple-exponential process, Figure 4, and our initial analysis (see Results) assumed a simple, single-step model. For this, the value of the association rate constant for all nucleotides was of the order of 10^4–$10^5\,M^{-1}\,s^{-1}$, substantially slower than the typical diffusion-controlled rate constants of 10^8–$10^9\,M^{-1}\,s^{-1}$. This discrepancy suggests our simple single-step model is incorrect, and that nucleotide binding is accompanied by an additional step such as a conformational change (Figure 8(a)). Data were reanalyzed to a model in which the formation of a diffusion-controlled encounter complex is followed by a conformational change. If the equilibrium constant of the diffusion-controlled encounter complex is K_1, and the forward and reverse rate constants for the second step are k_2 and k_{-2}, respectively, the observed rate constant for nucleotide binding can be described by:

$$k_{obs} = k_{-2} + \frac{k_2[ATP]}{K_1 + [ATP]}$$

As there is no curvature in the plots in Figure 4, K_1 must be greater than the maximum concentration of nucleotide used. Therefore, the equation reduces to:

$$k_{obs} = k_{-2} + \frac{k_2}{K_1}[ATP]$$

The slope of the plots will be k_2/K_1 (k_{on} in Table 1) and the intercept will be k_{-2} (k_{off} in Table 1). Hence, nucleotides bind *via* a two-step process: the initial diffusion-controlled binding is weak with a dissociation constant for ATP in the millimolar range and is followed by a conformational change with rate of formation greater than $250\,s^{-1}$. Such a conformational change could be the closure of the lid over the nucleotide-binding pocket. The role of this potential lid in the ATP mechanism remains intangible as structural studies of the isolated N-terminal domains have yet to show significant conformational switching from an open to a closed position.[6,14,28,29] This does not preclude the role of this lid region in ATP binding and hydrolysis as changes in the dynamics of this region on ATP binding have been observed by perturbation in the chemical shifts observed by NMR.[29]

The presence of an intermediate step involving a conformational change between the initial formation of an enzyme–substrate complex and the rate-determining step is not precluded by the lack of any difference between K_m and K_d, which we found to be equal within error (200 μM). As k_{-2}, the reverse rate constant for the conformational change after ATP binding ($9\,s^{-1}$) is much greater than k_3, the hydrolysis rate ($9\times10^{-5}\,s^{-1}$) theory predicts

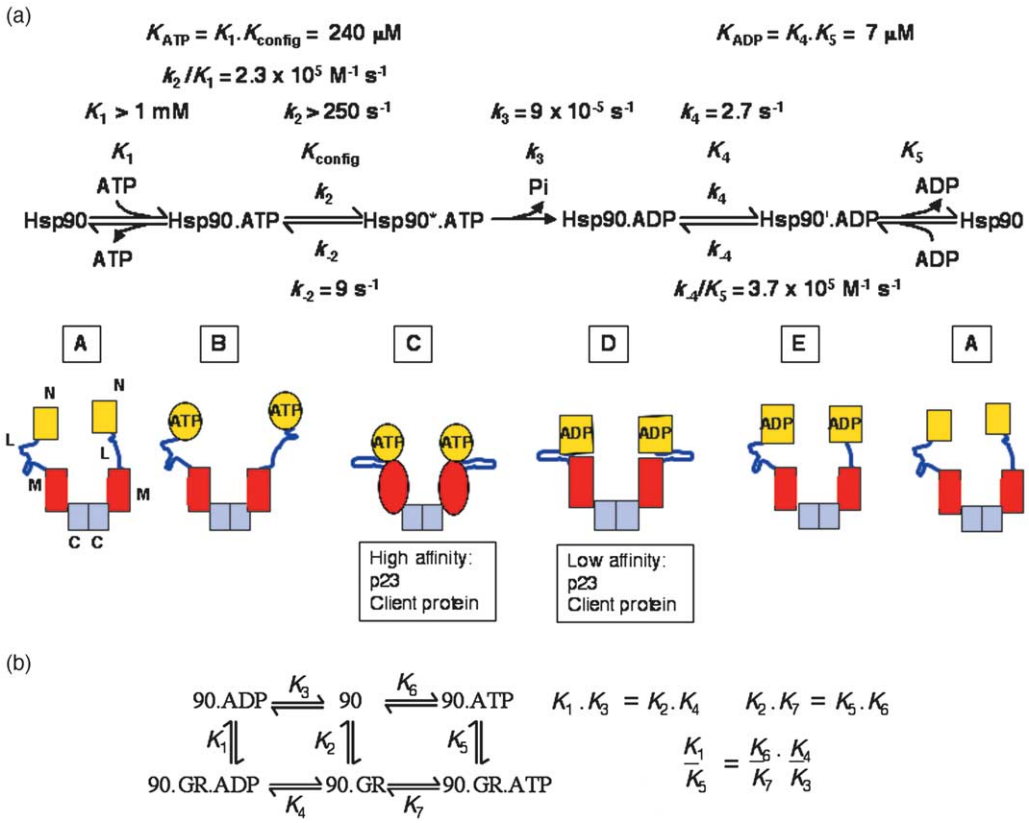

Figure 8. Kinetic model of human Hsp90 ATPase cycle. (a) ATP binds rapidly to Hsp90 under diffusion control (A to B). The binding of ATP in state B is weak with an equilibrium constant in the millimolar range. ATP binding induces a conformational change, possibly involving the "ATP-lid" in the N-terminal domain and/or contact between the N and M domain (B to C). However, the precise conformational changes that occur are unknown at present. The ATP-bound conformation of Hsp90 has a high affinity for client proteins and the co-chaperone p23. The rate-limiting step is the hydrolysis of ATP (C to D) possibly involving re-arrangement of a catalytic loop in the M domain. The ADP-bound state D has a lower affinity for both client and p23. Rapid dissociation of ADP allows recycling of Hsp90. (b) Thermodynamic linkage of client protein binding and nucleotide affinity allows the effect of nucleotide on the Hsp90–client protein affinity to be calculated.

that K_m is equal to K_d which is a product of K_1 and K_2. In contrast, a previous study of yeast Hsp90 nucleotide binding identified such a difference with the K_d of 500 μM, being approximately five times the value measured for K_m.[17] It is possible that the two Hsp90s have different kinetic mechanisms. However, given the sequence identity between the yeast and human proteins (64%), it will be illuminating to examine the kinetics of yeast Hsp90 in further detail.

N-terminal dimerisation of human Hsp90

In contrast to the parabolic dependence of activity on protein concentration observed in kinetic studies of the other GHKL ATPase family members such as DNA Gyrase B[26] and eukaryotic DNA topoisomerase II,[30] monomeric C-terminally truncated human Hsp90 showed a linear dependence on protein concentration over the range studied. Together with the lack of cooperativity in nucleotide binding and hydrolysis, we have no evidence which supports an N-terminal dimerisation step.

Although weak ATP-dependent cross-linking of fragments of Hsp90 has been shown,[7] it is not known if this reflects N-terminal dimerisation as the position of interacting elements has not been resolved. As ATP binding is coupled to conformational changes in other domains resulting in client and co-chaperone binding,[15] it is possible that, in their absence, the naked Hsp90 subunits may be free to transiently interact *via* these unoccupied surfaces. For example, ATP could induce changes in the flexibility of a loop in the middle domain predicted to be a possible client protein interaction site.[19] As this loop contains multiple lysine residues, an amine-specific cross-linker will modify and could cross-link to other subunits non-specifically. Similarly, correlations between the levels of cross-linking and the ATPase rates of mutants, engineered to change the dynamics of the ATP-lid, may only reflect ATP-induced conformational changes in other domains rather than a dimerisation of the N-terminal domains. ATP binding is certainly linked to conformational changes as we have shown here. Where the conformation changes occur, however, are uncertain.

Table 1. Kinetic and thermodynamic parameters of Hsp90 ATPase activity

Protein	T (°C)	Ligand	K_d (μM)	K_m (μM)	k_{on} ($M^{-1}\,s^{-1}$)	k_{off} (s^{-1})	$K_{d\ kin}$ (μM)	k_{hyd} (s^{-1})	k_{cat} (s^{-1})
Human Hsp90	10	AMP-PNP	106±7		$5.6(\pm0.1)\times10^{4}$	4.5±0.7	80±13		
Human Hsp90	10	ATP	284±26		$1.0(\pm0.1)\times10^{5}$	16.3±2.3	161±24		
Human Hsp90	25	AMP-PNP	148±12						
Human Hsp90+GR	25	AMP-PNP	7.4±0.9						
Human Hsp90	25	ATP	240±14	190±20	$2.3(\pm0.1)\times10^{5}$	9.0±3.0	39±13	$7(\pm1)\times10^{-5}$	$9.2(\pm0.2)\times10^{-5}$
Human Hsp90+GR	25	ATP	15±1						
Human Hsp90	25	ADP	7.2±0.3						
Human Hsp90	25	ADP	11±2		$3.7(\pm0.1)\times10^{5}$	2.7±1.6	7.2±1.6		
Human Hsp90+GR	25	ADP	41±6						
Human Hsp90	37	ATP		840±60[a]					$1.5(\pm0.1)\times10^{-3}$ [a]
Human Hsp90	37	AMP-PNP	790±45						
Human Hsp90	37	ADP	41±4						
Human Hsp90ΔC	25	AMP-PNP	80±40						
Human Hsp90ΔC	37	ATP		230±10					$1.2(\pm0.5)\times10^{-4}$
Yeast Hsp90	25	ATP	132±47[b]	100[c]			500[c]		
Yeast Hsp90	25	ADP	9±3[b]				150[c]	1.5×10^{-3} [c]	1.6×10^{-3} [c]
Yeast Hsp90	25	MABA-ATP			$1.6(\pm0.3)\times10^{5}$ [c]	2.9±0.2[c]	18.0±0.7[c]		
	37	ATP							1.3×10^{-2} [d]

[a] Data from the work done by McLaughlin *et al.*[10]
[b] Data from the work done by Prodromou *et al.*[28]
[c] Data from the work done by Weikl *et al.*[17]
[d] Data from the work done by Prodromou *et al.*[7]

It is pertinent that dimerisation of the N-terminal domain fragment alone was not evident after cross-linking[7] or even at the high concentrations used in NMR experiments.[29] As only a small fraction of Hsp90 was seen to form a doubly dimerised ring-structure by EM,[31] such a significant conformational switch has not yet been verified by a more detailed structural analysis. A recent small-angle X-ray scattering (SAXS) study on human Hsp90[32] did not detect any gross changes in the shape of human Hsp90 on ATP binding that N-terminal dimerisation would predict. If ATP binding drives N-terminal dimerisation, it would be expected that the energy of ATP binding in both domains needs to be transduced into a conformational rearrangement. So, it is perhaps significant that heterodimers formed between wild-type yeast Hsp90 and a point mutant (D79N) that fails to bind ATP is as active in ATP hydrolysis as the homodimeric wild-type.[33]

The nucleotide dependence of the interaction of client proteins with Hsp90

As the activation of client proteins involves a complex cycle with multiple chaperones and co-chaperones,[1,2] the effect of nucleotide status on the affinity of Hsp90 for client proteins is difficult to discern from other potential ATP-dependent processes such as co-chaperone association. For example, while the nucleotide status of Hsp90 has no effect on its affinity for the glucocortiocoid receptor,[34] the affinity for the structurally homologous progesterone receptor is dependent on ATP, with optimal binding within the range of the K_m (0.5–1 mM).[35] In another study, turnover of ATP was shown to be important to release GR-LBD from Hsp90 with mutants with reduced rates of ATP hydrolysis exhibiting slower rates of dissociation.[20]

To try to resolve the conflicting evidence, we took advantage of the observed effect of client protein on the nucleotide-binding affinity of Hsp90. It follows that nucleotide binding and client protein binding are thermodynamically linked. Figure 8 shows how such a relationship allows the change in nucleotide affinity to be used to calculate the relative affinities for client protein in the presence of ATP and ADP. Using the data at 25 °C, the ATP-bound state of Hsp90 is calculated to have approximately a 90-fold higher affinity for client protein than the ADP-state.

In the cell, the proportion of Hsp90 in the ATP state depends upon the relative affinities for nucleotide and the total free concentrations of ATP and ADP. If the free concentration of ATP is approximately 2 mM[36] with a free ADP concentration of approximately 15–40 μM,[37,38] the ATP form will be between two- and sevenfold more abundant than the ADP form. Hence, we propose that the ATP-bound form of Hsp90 will be the acceptor for client proteins. As the ADP interaction is much tighter than that for ATP (41 μM and 840 μM, respectively), Hsp90 is more sensitive to fluctuations in ADP concentration. It is interesting to speculate whether, under heat shock or cellular stress, any increase in the free ADP concentrations would cause a shift in the function of Hsp90 by decreasing its affinity for client proteins thereby releasing it to act as a non-ATP dependent general molecular chaperone.

Functional significance of ATP kinetics

From our observations on the nucleotide affinity and kinetics of ATP hydrolysis, we propose a model for Hsp90 function (Figure 8). In the absence of nucleotide, Hsp90 is in a flexible state. ATP binding in the N-terminal domain of Hsp90 causes a conformational switch, that may be transduced by docking of the N and middle domains, to a high affinity-state for client proteins and the co-chaperone p23. We have shown that the rate-limiting step is the hydrolysis of ATP which involves movement of a catalytic loop in the middle domain towards the nucleotide-binding site in the N-terminal domain.[19,39] The slower rate of hydrolysis seen in human Hsp90 may reflect reduced loop dynamics. The lower activity of the monomeric Hsp90ΔC may reflect a regulatory effect of the C-terminal domain on ATPase activity.[40] Interaction of Hsp90 with a client protein accelerates the rate-limiting hydrolysis step, converting Hsp90 into its ADP-state that has low affinity for both client proteins and p23. The rapid dissociation of ADP after hydrolysis returns Hsp90 to its original state. In the presence of p23, the ATPase activity is inhibited,[10] increasing the longevity of the high-affinity ATP state. Hence, the time that a client protein remains bound will depend on the rate of ATP hydrolysis in the Hsp90 complex. It should be emphasised that, as the ATPase activity between the domains are not linked, both subunits are not synchronised. Hence, Hsp90 does not have to undergo symmetrical conformational changes in both subunits concurrently during the ATP cycle.

The advantage for such an "open-ring" mechanism is the conformational flexibility allowed in the interaction with client proteins. Evidence suggests that it is likely that Hsp90 binds to highly structured client proteins, such as the GR-LBD,[41] the size and properties of the client protein surface will determine the nature of the interaction. The challenge of forming complexes with a diverse clientele may be the reason Hsp90 can recognise multiple discrete segments in client proteins,[42] suggesting there are multiple client interaction sites. If Hsp90 formed an N-terminal dimerised molecular clamp like DNA Gyrase B, where the client protein would be encapsulated between the two subunits of Hsp90, the internal diameter of the space occupied by the client protein would be only approximately 20 Å. Such a distance would be too small to accommodate the range of client proteins whose structures are known such as GR-LBD (1M2Z), cdk6 (1BLX), the kinase domain of human lymphocyte kinase (3LCK) and PKB/Akt (106K). In these cases, the walls of the Hsp90 clamp would have to be up to

50 Å apart. Instead, an appropriate distance to allow client protein sequestration could be maintained by co-chaperone binding. For example, the kinase specific co-chaperone cdc37 binds as a dimer to the N-terminal domains of Hsp90,[32,43] so facilitating loading of the kinase onto Hsp90 not only by targeting the bound kinase client protein to Hsp90 but by creating a distance of over 40 Å between the two subunits. The co-chaperone p23 may fulfill a similar role for other client proteins such as the steroid hormone receptors since it too has been found to bind to both subunits of Hsp90.[44] Bridging of the subunits may be necessary for the asymmetric binding of some client proteins to different sites in each subunit. In the absence of a mandatory N-terminal dimerisation mechanism, Hsp90 could form an open platform containing two ATP-dependent client protein sites for other client proteins. This could facilitate Hsp90's function as a matchmaker for assembly by binding multiple client proteins such as p53 and mdm2[45] or eNOS and PKB/Akt.[46] Thus, without the conformational restriction linking the N-terminal domains for activity, the molecular chaperone Hsp90 may hold within its subunits a diverse set of client proteins without discriminating on the basis of shape or size.

Methods

Protein expression and purification

Human Hsp90β and human GR-LBD were expressed and purified as described.[10,41] Hsp90ΔC was generated by introducing a stop codon at 1696 by site-directed mutagenesis (QuikChange, Stratagene). Human Hsp90ΔC was expressed and purified as described for full-length Hsp90 using a combination of nickel-iminodiacetic acid agarose (Sigma), ion exchange (MonoQ HR10/10, Pharmacia) and gel filtration (G75 Sephadex HR26/60, Pharmacia) with the inclusion of 10% glycerol to the final purified protein. The purity of the proteins was determined by SDS-PAGE, mass spectrometry and N-terminal protein sequencing to be greater than 95% (data not shown). Protein concentrations were determined spectrophotometrically and quoted as monomers.

Isothermal titration calorimetry

Isothermal titration calorimetry was performed using a MicroCal VP-ITC instrument (Microcal Inc., Northampton, MA USA). Two hundred and fifty microlitres of 4.3 mM AMP-PNP in a syringe was injected into a 2.5 ml cell containing 55.2 μM Hsp90 in 50 mM Tris–HCl (pH 7.4), 6 mM $MgCl_2$ 20 mM KCl, 1 mM dithioreitol (DTT) (assay buffer) at 25 °C. Similarly 3.19 mM and 628 μM ADP were injected into 49 μM and 56.8 μM Hsp90, respectively. Parallel experiments were carried out by injecting nucleotide into assay buffer without Hsp90 to correct for the heat of dilution in subsequent data analysis using the Origin software package (MicroCal Inc.). Both protein and nucleotide concentrations were determined spectrophotometrically.

Steady-state nucleotide binding

Binding of increasing concentrations of ADP, ATP and AMP-PNP (Sigma) to 2 μM Hsp90 in assay buffer in the absence or presence of 2 μM GR-LBD was measured by fluorescence emission at 338 nm using a SLM Aminco Bowman Series 2 luminescence spectrometer using an excitation wavelength of 295 nm with excitation and emission band pass of 4 nm at 25(±0.1) °C. To correct for the apparent decrease in fluorescence of Hsp90 due to the inner-filter effect of absorption of incident light at 295 nm by nucleotide, the change in fluorescence of Hsp90 was corrected using:

$$F_{\mathrm{corr}} = \frac{F_{\mathrm{obs}}}{10^{-m[\mathrm{L}]}} \tag{1}$$

where [L] is the ligand concentration and m is a constant determined for ratios of F_{corr} and F_{obs} at saturating nucleotide concentrations (at least tenfold the dissociation constant). Using a single-binding site model, where the concentration of the Hsp90–ligand complex is directly proportional to the change in fluorescence (ΔF), the corrected data were fitted to the following equations:

$$\Delta F = \frac{\Delta F_{\mathrm{max}}[\mathrm{L}]}{K_{\mathrm{d}} + [\mathrm{L}]} \tag{2}$$

$$\Delta F = \Delta F_{\mathrm{max}} - K_{\mathrm{d}} \frac{\Delta F}{[\mathrm{L}]} \tag{3}$$

where K_{d} is the dissociation constant and [L] is the concentration of ligand. Using the values of ΔF_{max} derived from fits to equations (2) and (3), the data were transformed and fitted to a Hill equation to determine the cooperativity:

$$\log\left(\frac{\Delta F}{\Delta F_{\mathrm{max}} - \Delta F}\right) = n \log[\mathrm{L}] - \log K_{\mathrm{d}} \tag{4}$$

where n is the degree of cooperativity.

Pre-steady state nucleotide binding

An Applied Photophysics Stopped-Flow Reaction Analyser (model SF.17MV) was used and data were acquired and analysed using the Applied Photophysics Kinetic Workstation, version 4.099, supplied. Excitation was set at 295 nm with a cut-off filter of 320 nm. Hsp90 (10 μM) was mixed with increasing concentrations of nucleotides in assay buffer at 10 °C or 25(±0.1) °C.

ATPase activity

Steady-state ATP hydrolysis was measured by the relative fluorescence emission of A197C PBP-labelled with *N*-[2-(1-maleimidyl)ethyl]-7-(diethylamino)coumarin-3-carboxamide (MDCC, Molecular Probes) upon binding inorganic phosphate as described.[10,47] For steady-state experiments, 1 μM MDCC–PBP was used to measure the inorganic phosphate released by Hsp90 and Hsp90ΔC in assay buffer containing increasing concentrations of ATP at either 25 °C or 37 °C.

For single-turnover experiments, 100–200 μM ATP was added to 250 μM Hsp90 in assay buffer and incubated at 25 °C. A control reaction without Hsp90 was also incubated to measure the spontaneous rate of ATP hydrolysis. At times indicated, 2 μl of the reactions were quenched on ice with a final concentration of 20 mM ethylene diaminetetraacetic acid (EDTA). The concentration of inorganic phosphate released was measured

with 5 μM MDCC–PBP in 200 μl 50 mM Tris–HCl, pH 7.4. Data were fitted to:

$$A_t = A_0\left[1 - \exp(-kt)\right] \quad (5)$$

where A_0 is the concentration of the initial Hsp90.ATP complex formed calculated using the total concentrations and measured equilibrium constant, A_t is the concentration of inorganic phosphate released at time t and k is the first-order rate constant. All assays were carried out in triplicate.

Determination of the oligomeric state of Hsp90ΔC

Analytical size-exclusion experiments were performed on a Sephadex 200 HR10/30 (Pharmacia) column equilibrated in 50 mM Tris–HCl (pH 7.4), 150 mM NaCl, 6 mM $MgCl_2$, 20 mM KCl, 1 mM DTT, 1 mM ATP. The relative elution volume of 200 μl of between 10 μM and 70 μM Hsp90ΔC was compared with molecular weight standards (Sigma).

The relative elution volume was calculated as:

$$K_{AV} = \frac{V_e - V_o}{V_g - V_o} \quad (6)$$

where V_e is the elution volume, V_o is the void volume determined by elution of Blue Dextran 2000 (Sigma) and V_g is the geometric column volume.

Acknowledgements

We thank Professor Ernest Laue (Department of Biochemistry, University of Cambridge, UK) and Dr M. Shirouzu (Riken Institute, Japan) for the human Hsp90β plasmid and Dr Martin Webb (NIMR, Mill Hill, UK) for the gift of PBP expression vector. We acknowledge fruitful discussions with Dr Pam Rowling, Professor Ernest Laue, Dr Wei Zhang and Edward Coulstock. We are grateful to Jonathan Phillips for running mass spectrometry experiments, Ryan Bentley, Keith Jordan, Sheila McCann for technical assistance and Dr Chris Johnson and Professor Sir Alan Fersht (MRC Centre for Protein Engineering, Cambridge, UK) for advice on calorimetry experiments. This work was funded by a Leverhulme Special Research Fellowship (S.H.M.) and the Welton Foundation.

References

1. Pratt, W. B. (1998). The hsp90-based chaperone system: involvement in signal transduction from a variety of hormone and growth factor receptors. *Proc. Soc. Expt. Biol. Med.* **217**, 420–434.
2. Wegele, H., Muller, L. & Buchner, J. (2004). Hsp70 and Hsp90—a relay team for protein folding. *Rev. Physiol. Biochem. Pharmacol.* **151**, 1–44.
3. Picard, D. (2002). Heat-shock protein 90, a chaperone for folding and regulation. *Cell. Mol. Life Sci.* **59**, 1640–1648.
4. Young, J. C., Moarefi, I. & Hartl, F. U. (2001). Hsp90: a specialized but essential protein-folding tool. *J. Cell Biol.* **154**, 267–273.
5. Panaretou, B., Prodromou, C., Roe, S. M., O'Brien, R., Ladbury, J. E., Piper, P. W. & Pearl, L. H. (1998). ATP binding and hydrolysis are essential to the function of the Hsp90 molecular chaperone *in vivo*. *EMBO J.* **17**, 4829–4836.
6. Obermann, W. M. J., Sondermann, H., Russo, A. A., Pavletich, N. P. & Hartl, F. U. (1998). *In vivo* function of Hsp90 is dependent on ATP binding and ATP hydrolysis. *J. Cell Biol.* **143**, 901–910.
7. Prodromou, C., Panaretou, B., Chohan, S., Siligardi, G., O'Brien, R., Ladbury, J. E. *et al*. (2000). The ATPase cycle of Hsp90 drives a molecular "clamp" *via* transient dimerization of the N-terminal domains. *EMBO J.* **19**, 4383–4392.
8. Prodromou, C., Siligardi, G., O'Brien, R., Woolfson, D. N., Regan, L., Panaretou, B. *et al*. (1999). Regulation of Hsp90 ATPase activity by tetratricopeptide repeat (TPR)-domain co-chaperones. *EMBO J.* **18**, 754–762.
9. Panaretou, B., Siligardi, G., Meyer, P., Maloney, A., Sullivan, J. K., Singh, S. *et al*. (2002). Activation of the ATPase activity of hsp90 by the stress-regulated cochaperone Aha1. *Mol. Cell*, **10**, 1307–1318.
10. McLaughlin, S. H., Smith, H. W. & Jackson, S. E. (2002). Stimulation of the weak ATPase activity of human Hsp90 by a client protein. *J. Mol. Biol.* **315**, 787–798.
11. Richter, K., Muschler, P., Hainzl, O., Reinstein, J. & Buchner, J. (2003). Sti1 is a non-competitive inhibitor of the Hsp90 ATPase. Binding prevents the N-terminal dimerization reaction during the ATPase cycle. *J. Biol. Chem.* **278**, 10328–10333.
12. Stebbins, C. E., Russo, A. A., Schneider, C., Rosen, N., Hartl, F. U. & Pavletich, N. P. (1997). Crystal structure of an Hsp90-geldanamycin complex: targeting of a protein chaperone by an antitumor agent. *Cell*, **89**, 239–250.
13. Basso, A. D., Solit, D. B., Chiosis, G., Giri, B., Tsichlis, P. & Rosen, N. (2002). Akt forms an intracellular complex with heat shock protein 90 (Hsp90) and Cdc37 and is destabilized by inhibitors of Hsp90 function. *J. Biol. Chem.* **277**, 39858–39866.
14. Prodromou, C., Roe, S. M., Piper, P. W. & Pearl, L. H. (1997). A molecular clamp in the crystal structure of the N-terminal domain of the yeast Hsp90 chaperone. *Nature Struct. Biol.* **4**, 477–482.
15. Sullivan, W., Stensgard, B., Caucutt, G., Bartha, B., McMahon, N., Alnemri, E. S. *et al*. (1997). Nucleotides and two functional states of Hsp90. *J. Biol. Chem.* **272**, 8007–8012.
16. Dutta, R. & Inouye, M. (2000). GHKL, an emergent ATPase/kinase superfamily. *Trends Biochem. Sci.* **25**, 24–28.
17. Weikl, T., Muschler, P., Richter, K., Veit, T., Reinstein, J. & Buchner, J. (2000). C-terminal regions of Hsp90 are important for trapping the nucleotide during the ATPase cycle. *J. Mol. Biol.* **303**, 583–592.
18. Wigley, D. B., Davies, G. J., Dodson, E. J., Maxwell, A. & Dodson, G. (1991). Crystal structure of an N-terminal fragment of the DNA Gyrase B protein. *Nature*, **351**, 624–629.
19. Meyer, P., Prodromou, C., Hu, B., Vaughan, C., Roe, S. M., Panaretou, B. *et al*. (2003). Structural and functional analysis of the middle segment of Hsp90. Implications for ATP hydrolysis and client protein and cochaperone interactions. *Mol. Cell*, **11**, 647–658.
20. Young, J. C. & Hartl, F. U. (2000). Polypeptide release by Hsp90 involves ATP hydrolysis and is enhanced by the co-chaperone p23. *EMBO J.* **19**, 5930–5940.
21. Garnier, C., Lafitte, D., Tsvetkov, P. O., Barbier, P.,

Leclerc-Devin, J., Millot, J. M. *et al*. (2002). Binding of ATP to heat shock protein 90: evidence for an ATP-binding site in the C-terminal domain. *J. Biol. Chem.* **277**, 12208–12214.
22. Soti, C., Racz, A. & Csermely, P. (2002). A nucleotide-dependent molecular switch controls ATP binding at the C-terminal domain of Hsp90·N-terminal nucleotide binding unmasks a C-terminal binding pocket. *J. Biol. Chem.* **277**, 7066–7075.
23. Marcu, M. G., Chadli, A., Bouhouche, I., Catelli, M. & Neckers, L. M. (2000). The heat shock protein 90 antagonist novobiocin interacts with a previously unrecognized ATP-binding domain in the carboxyl terminus of the chaperone. *J. Biol. Chem.* **275**, 37181–37186.
24. Adair, G. S. (1925). The hemoglobin system. VI The oxygen dissociation curve of hemoglobin. *J. Biol. Chem.* **63**, 529–545.
25. Ban, C., Junop, M. & Yang, W. (1999). Transformation of MutL by ATP binding and hydrolysis: a switch in DNA mismatch repair. *Cell*, **97**, 85–97.
26. Brino, L., Urzhumtsev, A., Mousli, M., Bronner, C., Mitschler, A., Oudet, P. & Moras, D. (2000). Dimerization of *Escherichia coli* DNA-Gyrase B provides a structural mechanism for activating the ATPase catalytic center. *J. Biol. Chem.* **275**, 9468–9475.
27. McLaughlin, S. H. & Bulleid, N. J. (1998). Thiol-independent interaction of protein disulphide isomerase with type X collagen during intra-cellular folding and assembly. *Biochem. J.* **331**, 793–800.
28. Prodromou, C., Roe, S. M., O'Brien, D. N., Ladbury, J. E., Piper, P. W. & Pearl, L. H. (1997). Identification and structural characterization of the ATP/ADP-binding site in the Hsp90 molecular chaperone. *Cell*, **90**, 65–75.
29. Dehner, A., Furrer, J., Richter, K., Schuster, I., Buchner, J. & Kessler, H. (2003). NMR chemical shift perturbation study of the N-terminal domain of Hsp90 upon binding of ADP, AMP-PNP, Geldanamycin, and Radicicol. *Chembiochem*, **4**, 870–877.
30. Hu, T., Sage, H. & Hsieh, T. S. (2002). ATPase domain of eukaryotic DNA topoisomerase II. Inhibition of ATPase activity by the anti-cancer drug bisdioxopiperazine and ATP/ADP-induced dimerization. *J. Biol. Chem.* **277**, 5944–5951.
31. Maruya, M., Sameshima, M., Nemoto, T. & Yahara, I. (1999). Monomer arrangement in HSP90 dimer as determined by decoration with N and C-terminal region specific antibodies. *J. Mol. Biol.* **285**, 903–907.
32. Zhang, W., Hirshberg, M., McLaughlin, S. H., Lazar, G. A., Nielsen, P. R., Sobott, F. *et al*. (2004). Biochemical and structural studies of the interaction of cdc37 with Hsp90. *J. Mol. Biol.* **240**, 891–907.
33. Richter, K., Muschler, P., Hainzl, O. & Buchner, J. (2001). Coordinated ATP hydrolysis by the Hsp90 dimer. *J. Biol. Chem.* **276**, 33689–33696.
34. Kanelakis, K. C., Shewach, D. S. & Pratt, W. B. (2002). Nucleotide binding states of hsp70 and hsp90 during sequential steps in the process of glucocorticoid receptor.hsp90 heterocomplex assembly. *J. Biol. Chem.* **277**, 33698–33703.
35. Kosano, H., Stensgard, B., Charlesworth, M. C., McMahon, N. & Toft, D. (1998). The assembly of progesterone receptor–Hsp90 complexes using purified proteins. *J. Biol. Chem.* **273**, 32973–32979.
36. Gribble, F. M., Loussouarn, G., Tucker, S. J., Zhao, C., Nichols, C. G. & Ashcroft, F. M. (2000). A novel method for measurement of submembrane ATP concentration. *J. Biol. Chem.* **275**, 30046–30049.
37. Ronner, P., Friel, E., Czerniawski, K. & Frankle, S. (1999). Luminometric assays of ATP, phosphocreatine, and creatine for estimation of free ADP and free AMP. *Anal. Biochem.* **275**, 208–216.
38. Ghosh, A., Ronner, P., Cheong, E., Khalid, P. & Matschinsky, F. M. (1991). The role of ATP and free ADP in metabolic coupling during fuel-stimulated insulin release from islet beta-cells in the isolated perfused rat pancreas. *J. Biol. Chem.* **266**, 22887–22892.
39. Meyer, P., Prodromou, C., Liao, C., Hu, B., Mark Roe, S., Vaughan, C. K. *et al*. (2004). Structural basis for recruitment of the ATPase activator Aha1 to the Hsp90 chaperone machinery. *EMBO J.* **6**, 1402–1410.
40. Owen, B. A. L., Sullivan, W. P., Felts, S. J. & Toft, D. O. (2002). Regulation of heat shock protein 90 ATPase activity by sequences in the carboxyl terminus. *J. Biol. Chem.* **277**, 7086–7091.
41. McLaughlin, S. H. & Jackson, S. E. (2002). Folding and stability of the ligand-binding domain of the glucocorticoid receptor. *Protein Sci.* **11**, 1926–1936.
42. Scroggins, B. T., Prince, T., Shao, J., Uma, S., Huang, W., Guo, Y. *et al*. (2003). High affinity binding of Hsp90 is triggered by multiple discrete segments of its kinase clients. *Biochemistry*, **42**, 12550–12561.
43. Roe, S. M., Ali, M. M., Meyer, P., Vaughan, C. K., Panaretou, B., Piper, P. W. *et al*. (2004). The mechanism of Hsp90 regulation by the protein kinase-specific cochaperone p50(cdc37). *Cell*, **116**, 87–98.
44. Chadli, A., Bouhouche, I., Sullivan, W., Stensgard, B., McMahon, N., Catelli, M. G. & Toft, D. O. (2000). Dimerization and N-terminal domain proximity underlie the function of the molecular chaperone heat shock protein 90. *Proc. Natl Acad. Sci. USA*, **97**, 12524–12529.
45. Peng, Y. H., Chen, L. H., Li, C. G., Lu, W. G. & Chen, J. D. (2001). Inhibition of MDM2 by hsp90 contributes to mutant p53 stabilization. *J. Biol. Chem.* **276**, 40583–40590.
46. Fontana, J., Fulton, D., Chen, Y., Fairchild, T. A., McCabe, T. J., Fujita, N. *et al*. (2002). Domain mapping studies reveal that the M domain of hsp90 serves as a molecular scaffold to regulate Akt-dependent phosphorylation of endothelial nitric oxide synthase and NO release. *Circ. Res.* **90**, 866–873.
47. Brune, M., Hunter, J. L., Corrie, J. E. T. & Webb, M. R. (1994). Direct, real-time measurement of rapid inorganic-phosphate release using a novel fluorescent-probe and its application to actomyosin subfragment-1 ATPase. *Biochemistry*, **33**, 8262–8271.

Edited by F. Schmid

(Received 27 May 2004; received in revised form 16 August 2004; accepted 20 September 2004)